

## Natural Fracture Characterization from Microseismic Source Mechanisms: A Comparison with FMI Data

*Jo Ellen Kilpatrick\*, Leo Eisner, Sherilyn Williams-Stroud, Brian Cornette Microseismic Inc., Morris Hall, Williams*

### Summary

Microseismic monitoring of hydraulic fracture stimulations is used to determine the extent of fractured rock resulting from the treatment by mapping the locations of induced microseismic events. Usually the geometry of the event locations is used to infer fracture orientations; e.g. trends of microseismic events concentrated along a particular azimuth (or with a planar distribution in 3D) can indicate fracturing along a plane with that orientation. In this study we use additional parameters extracted from induced microseismic events (source mechanisms) to determine the specific fracturing behavior and compare them with independent observations from an FMI log in the treatment well. In a horizontal well located in the mid-Continental USA, we present the results of source mechanism analysis for the best signal-to-noise events triggered by the fracture stimulation treatment. The microseismic events with source mechanisms have failure planes with very similar orientations to natural fractures in the image log. Our results are consistent with the reactivation of natural fractures during the stimulation treatment, suggesting that it is possible to determine natural fracture orientations in the reservoir in cases where image logs are not available. In addition, the microseismic event source mechanisms allow fracture characterization away from the wellbore, providing critical constraints for building fractured reservoir models.

### Introduction

Upscaling or downscaling of measured data is a formidable challenge in characterization of reservoir properties and significant assumptions need to be made in order to bridge measurements that were acquired on different scales. This is particularly true for correlating wellbore measurements and seismic measurements (e.g. Prioul and Jocker, 2009). A successful characterization of natural fractures plays an important role in modeling fluid transport through reservoir formation. Analysis of in-situ data from borehole images (e.g. FMI or acoustic image logs) is commonly done to identify the presence and orientations of natural fractures (Wu and Pollard, 2002). Measurements made at the borehole are usually extrapolated to larger scale properties such as seismic anisotropy or coherence in order to characterize reservoir properties between boreholes (Lees, 1998). As fractures are a natural chaotic system associated with significant spatial variability, a key question in those extrapolations is the feasibility of extrapolating

measurements of fractures from wellbores on the centimeter scale to fractures in the reservoir with a length scale of hundreds of meters.

Rutledge and Phillips (2003) proposed that the orientation of natural fractures controls orientations of failure planes of induced microseismic events. In their model, small-scale natural fractures coalesce to form larger faults of several meters. They observed strike-slip source mechanisms on vertical failure planes for induced microseismic events striking nearly parallel to natural fractures in Cotton Valley rocks (Dutton et al, 1991). However, because Rutledge and Phillips observations were based on inversion from a small number of geophones in two monitoring boreholes, they were able to determine only a composite (average) focal mechanism from many events grouped on the assumption of mechanism similarity, raising significant doubts about the accuracy of the observed results (e.g. Sileny et.al. 2009).

### Case Study

Surface based microseismic monitoring was done to assess the effectiveness of two different fluids used for fracture stimulations in a horizontal well with a 3500' lateral drilled in the Arkoma Basin of Oklahoma. Slick-water was used to treat the well from the toe to mid lateral. Nitrogen was used to treat the well from mid lateral to the heel. The monitoring array consisted of 1078 stations of 12 geophones, laid out in a radial pattern around the treatment well. The geophones were buried to a depth of one foot to maximize the signal to noise ratio by reducing the interference of the frequent seasonal rainfall. Cultural sources of noise such as traffic and inherent pad noises were taken into account by the surface array design and the seismic processing. A total of 25 hours of data were recorded and processed. Microseismic events induced by the hydraulic fracturing were located by a beamforming process, which is essentially a one-way depth migration. A layered velocity model was calculated using the perforation shots from each treatment as sources for calibration events. By taking a measurement of the arrival times across the array and plotting them against the distance between receivers, a velocity estimate from the well depth to the surface was derived. The derived velocities were consistent with RMS velocities calculated from a sonic log of the well bore. Receiver statics were then calculated from the perforation shot arrivals and used to complete the

## Microseismic and FMI characterize natural fractures

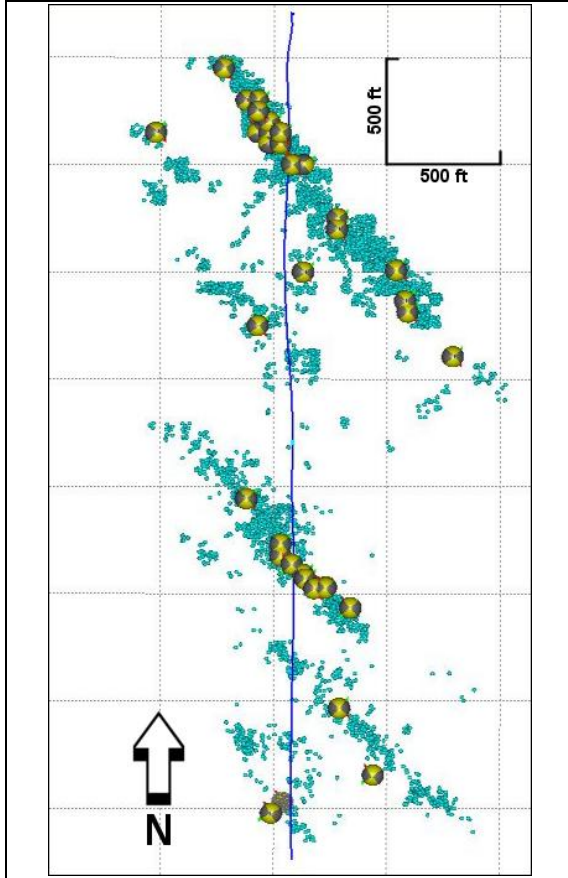


Figure 1: Map view of microseismic events showing locations of source mechanisms. The cyan dots show microseismic event locations. Yellow quadrants on the source mechanism beach balls represent compression, gray areas are tension. Grid line interval is 500 feet.

calibration of the model. Using the calibrated model, the events corresponding to the perforation shots located to within 50 feet of their measured location in the well bore. 44 highest signal to-noise ratio events at the reservoir level were inverted for their source mechanisms (Hall and Kilpatrick, 2009). The observed distribution of microseismic events created by the stimulation treatments suggested that planar fractures were created with varying complexity (Fig. 1). The azimuths of the produced trends correlate with the azimuth of natural fractures interpreted from the FMI logging on the well prior to treatment.

### Source mechanism inversion

We use source mechanism inversion from the surface data based on a least squares inversion of the observed P-wave amplitudes recorded on the vertical components of

recording geophones. The inversion algorithm uses the same data to obtain the full moment inversion (i.e. including the volumetric part of the source mechanism), and double-couple (shear) mechanism. In both cases we assume a point source. The moment tensor representing the source mechanism can be inverted from a point source relationship between observed displacements on vertical component  $A$  and moment tensor components  $M_{jk}$ :

$$A = G_{3j,k} M_{jk} , \quad (1)$$

Where  $G_{3j,k}$  are vertical components of the Green's function derivative (Aki and Richard, 1980). Einstein's summation rules over  $j,k$  indexes applies. Equation (1) can be inverted by either least squares (Sipkin, 1982) or a grid search (grid search is possible only for pure shear source mechanism as non-shear source mechanisms have an infinite number of possible combinations of  $M_{jk}$ ).

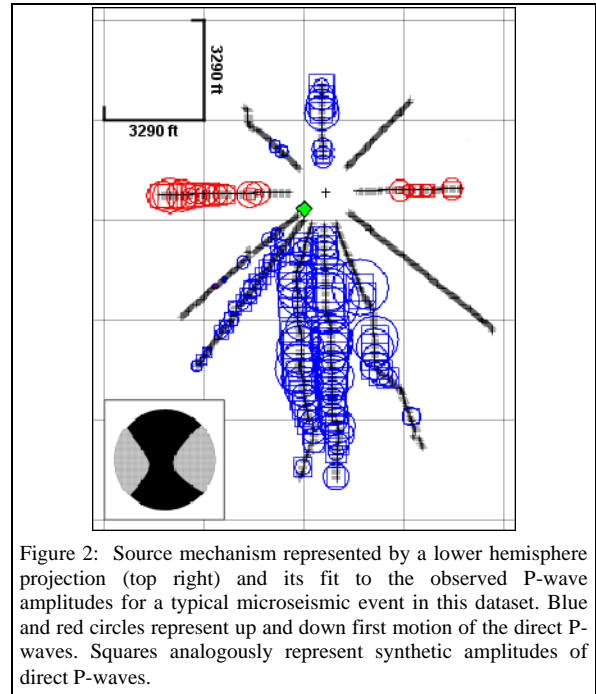


Figure 2: Source mechanism represented by a lower hemisphere projection (top right) and its fit to the observed P-wave amplitudes for a typical microseismic event in this dataset. Blue and red circles represent up and down first motion of the direct P-waves. Squares analogously represent synthetic amplitudes of direct P-waves.

Although in principle it is possible to use multiple waves observed at the surface (such as P- and S-waves), only amplitudes of direct P-waves on vertical receiver components are used for inversion of moment tensor in this study as they provide a robust inversion result independent of the poorly constrained S-wave velocity model. We used the Green's function derivatives in a homogeneous isotropic medium with correction for free surface and attenuation. Although heterogeneity of the velocities and

## Microseismic and FMI characterize natural fractures

densities affects source mechanism inversion, the broad distribution of receivers over multiple offsets and azimuths compensates for model heterogeneity and provides accurate estimates of fault plane orientations (see Šílený, 2009). This is further verified by a good fit of the observed modeled P-wave amplitudes in Figure 2.

In this dataset we observed microseismic events with both pure shear as well as more complex mechanisms. The more complex mechanisms can be characterized as tensile opening along nearly vertical fault planes with orientation very close to the events with pure shear mechanisms (Figure 3). Generalized inversion for six components of the moment tensor from broad azimuthal and offset coverage in four quadrants allowed us to determine reliably dips and strikes of the inverted fault planes even in the case of significant tensile components of the source mechanisms (Šílený, 2009). We have carried out a number of tests to investigate stability of the inverted results; in particular we have removed randomly approximately 10% of the receivers and repeated inversion for source mechanisms. We also tested the inversion by picking opposite arrival on receivers with weak signal-to-noise ratio. These tests resulted in minor changes to the inverted mechanism and variability of the inverted dips and strikes was at most 3-4°. Therefore we conclude that the inverted variations (5-10°) in strikes and dips of the fault planes represent true variation in source mechanism orientations and bin the inverted strikes and dips with 5° bins.

Note that the inverted mechanism of the representative events in Figure 2 is very close to pure strike-slip mechanism as 90% of the inverted moment is due to pure shear motion on along nearly vertical fault planes (dip 89° and 81°). Our results show that this mechanism provided ample energy to be accurately located, and that the assertion by Chambers et al (2010) that strike-slip events cannot be located from surface geophone arrays is incorrect. The accuracy of the location was further verified by moving out the seismic traces which flattened within 15 ms across the entire array. The corresponding seismic moment of the event shown in Figure 1 was approximately  $3.4 \cdot 10^7$  Nm, corresponding to magnitude -1.1.

### Fracture Analysis

The natural fracture orientations were identified in an image log acquired in the same well. Both drilling-induced and natural fractures were observed in the well, with the natural fracture orientation maximum at 84°/46° dip/dip azimuth (Fig. 3). The source mechanism solution planes are nearly identical to the orientations of natural fractures measured in the wellbore, and indicating that the existing natural fractures were reactivated during the treatment.

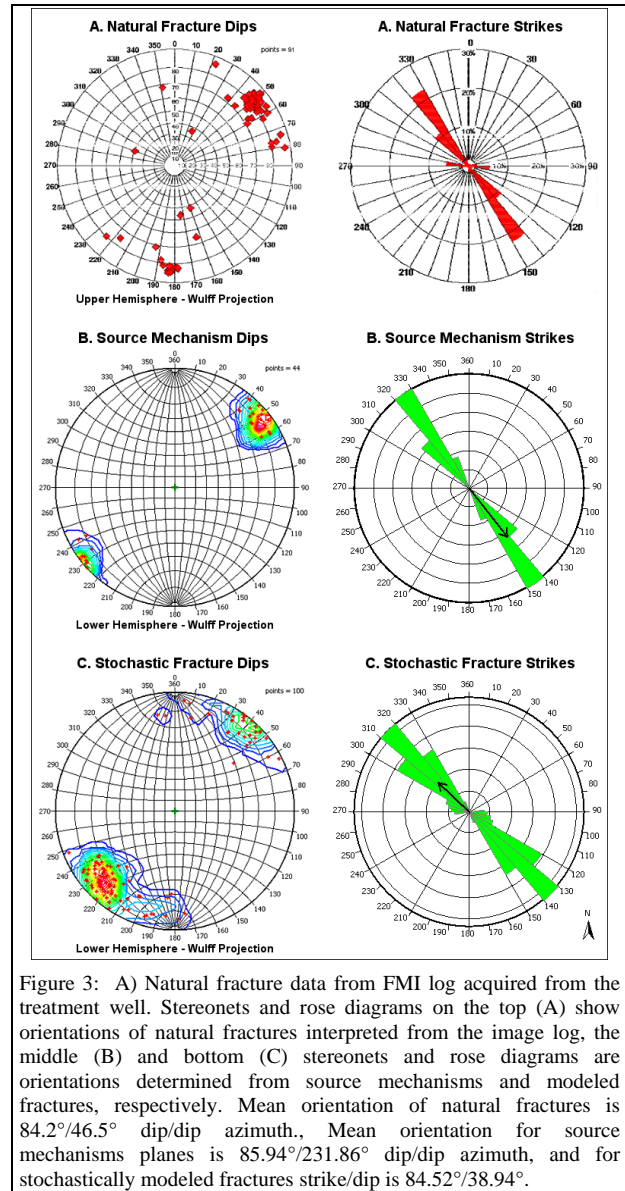


Figure 3: A) Natural fracture data from FMI log acquired from the treatment well. Stereonets and rose diagrams on the top (A) show orientations of natural fractures interpreted from the image log, the middle (B) and bottom (C) stereonets and rose diagrams are orientations determined from source mechanisms and modeled fractures, respectively. Mean orientation of natural fractures is 84.2°/46.5° dip/dip azimuth., Mean orientation for source mechanisms planes is 85.94°/231.86° dip/dip azimuth, and for stochastically modeled fractures strike/dip is 84.52°/38.94°.

Non-shear component of the inverted mechanisms is also present, indicating opening-mode failure mechanisms are also active, providing space where fracturing fluids and proppants could invade fault planes. Fractures interpreted in the image log include open and partially open natural fractures as well as drilling induced fractures with orientations that could be influenced by the existence of natural fractures. The in-situ stress indicators in the image log are primarily en-echelon tensile fractures oriented nearly E-W, but a few N-S breakouts are also identified. The source mechanisms indicate strike-slip reactivation of existing fractures. Observations of both types of borehole

## Microseismic and FMI characterize natural fractures

stress indicators (breakout and tensile fractures) have been reported in other wells where the tectonic stress regime is strike-slip (Barton et al, 1998). The perpendicular orientations of the breakouts and tensile fractures are consistent with their interpretations for the stress directions. The maximum horizontal stress direction of  $88^\circ$  azimuth from the drilling induced fractures is consistent with the stress directions required by the source mechanism inversion solutions, so that the same conclusion can be derived via either method.

Fracture characterization using explicitly determined locations and orientations of fractures through fault planes inverted from microseismic events allows a higher-resolution characterization away from the wellbore. We use the combination of source mechanisms and event locations to populate a geocellular model with fractures away from the wellbore. For events that were below the signal to noise threshold required to do the source mechanism inversion, a stochastic approach to generating fractures was applied. The stochastic approach also allows exploration of the larger location uncertainty associated with smaller events. Figure 4 shows one realization of a DFN (Discrete Fracture Network) model generated using this two-part approach. The wellbore image log analysis of the natural fracture orientations includes a secondary orientation maximum of steeply-dipping conductive natural fractures with a strike about  $10^\circ$  from the drilling induced fractures, (shown in Figure 3). These fractures are orientated so that they can be reactivated in shear in response to the in-situ stress, but will have a large tensile component than the NW-SE oriented natural fractures. The inclusion of these fractures in the DFN as a secondary set may provide the enhanced permeability required to achieve a history match using fracture flow properties calculated from the DFN. Although these fracture orientations are not resolved by source mechanism inversion, the knowledge of the geomechanical behavior of the reservoir obtained from the image log and the confirmation of reactivation of natural fractures from the inverted source mechanisms allows us to infer their mutual stimulation in areas of microseismicity. The result is a highly constrained upscaling of properties measured from the wellbore at a small scale and populated to the reservoir volume away from the well.

### Conclusions

In this study we use a unique opportunity to compare orientations of fault planes of individual microseismic events induced by hydraulic fracturing in a treatment well that has been logged with fractures in a borehole image log. The fault planes of individual microseismic events have similar strikes and dips as natural fractures observed in the

FMI log. This observation provides not only insight into the physics of the induced seismic events (reactivation of natural fractures) but also possibility of natural fracture characterization away from the wellbore which was previous to this primarily the domain of seismic anisotropy. This characterization is used to create a DFN of the reservoir rock based on deterministic fractures where locations and orientations are explicitly resolved and on stochastic fractures where events are detected, but their mechanisms are not determined. The result is reservoir property distribution based on the events that bridges the scales between reservoir and borehole data.

### Acknowledgements

Authors thanks Williams company for release of this dataset for publication.

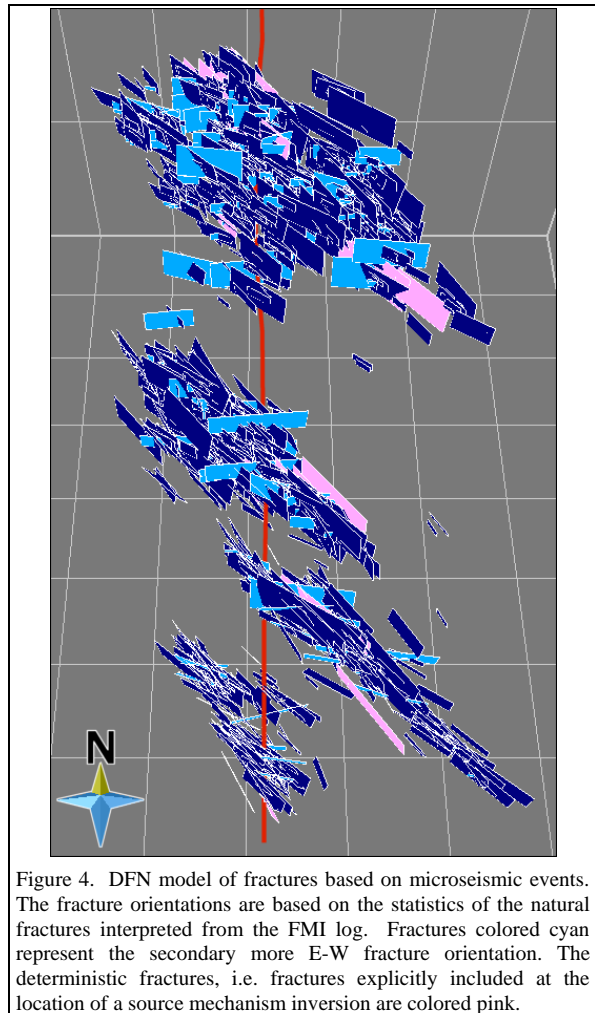


Figure 4. DFN model of fractures based on microseismic events. The fracture orientations are based on the statistics of the natural fractures interpreted from the FMI log. Fractures colored cyan represent the secondary more E-W fracture orientation. The deterministic fractures, i.e. fractures explicitly included at the location of a source mechanism inversion are colored pink.